Accelerated Publications

Characterization of the *Tetrahymena* Ribozyme Folding Pathway Using the Kinetic Footprinting Reagent Peroxynitrous Acid†

Steven G. Chaulk and Andrew M. MacMillan*

Department of Chemistry, University of Toronto, 80 St. George Street, Toronto, Ontario, Canada M5S 3H6

Received September 20, 1999; Revised Manuscript Received November 9, 1999

ABSTRACT: Large RNAs fold into complex structures which determine their biological activities. A full understanding of both RNA structure and dynamics will include the description of the pathways by which these structures are formed. Kinetic footprinting [Sclavi, B., et al. (1997) *J. Mol. Biol. 266,* 144−159] has been shown to be a powerful method for the study of dynamic processes involving RNA. Here we describe the use of a readily available reagent, peroxynitrous acid, as a kinetic footprinting tool for the study of RNA folding. Hydroxyl radicals generated from this reagent were used to footprint the *Tetrahymena* ribozyme during its magnesium-dependent folding—in agreement with synchroton X-ray footprinting [Sclavi, B., et al. (1998) *Science 279,* 1940−1943] and oligonucleotide/hybridization cleavage experiments [Zarrinkar, P. P., and Williamson, J. R. (1994) *Science 265,* 918−924], this work suggests an ordered, hierarchical folding pathway for the ribozyme. Several slow steps in the folding pathway were observed in the peroxynitrous acid footprinting, but none of these corresponded to the rate-determining step of folding. This suggests that the formation of the global, protected structure is followed by one or more slow local rearrangements to yield the final active structure. These studies illustrate the utility of peroxynitrous acid as a reagent for the elucidation of RNA folding pathways and the study of RNA dynamics.

RNA molecules are essential components of the biochemical machines which are responsible for translation, tRNA maturation, and RNA splicing (*1*). The unique three-dimensional structures adopted by these RNAs determine their activity, and thus an understanding of structure is key to a full appreciation of their biological roles. In some cases, such as the assembly of the spliceosome, a dynamic series of rearrangements of RNA structure is required to assemble an active catalytic complex. Considerable progress has been made in understanding the two- and three-dimensional structures adopted by large RNAs using phylogenetic, X-ray, NMR, and chemical probing techniques (*2*−*7*). The mechanisms and pathways by which large RNAs fold into these structures are obviously of interest, and there is a need for novel approaches to study these processes.

Recently, there has been considerable interest in the development of techniques to explore dynamic changes in RNA molecules such as folding or conformational rearrangements (*8*−*12*). The L-21 *Sca*I ribozyme has been used as a model system in many such studies because it has been extensively characterized biochemically and because high-resolution X-ray structures of several large fragments have been determined (*3, 4*). Phylogenetic comparisons (*2*) were originally used to predict a number of conserved paired regions (P) linked by joining (J) sequences providing a two-dimensional map of the ribozyme structure (Figure 1A)—the folding of the RNA into its active three-dimensional structure is a magnesium-dependent process producing a compact structure of tightly packed helical regions (*3, 4*).

Williamson and co-workers have used an oligonucleotide hybridization/RNase H cleavage assay to explore the magnesium-dependent folding pathways of the L-21 *Sca*I Group I ribozyme and also RNase P from *B. subtilis* and *E. coli.* (*8, 9*). In both cases, differential sensitivity to oligonucleotide hybridization and subsequent cleavage by RNase H were used to infer a hierarchy of intermediates along a folding pathway.

One of the most powerful techniques for probing nucleic acid structure is chemical footprinting with hydroxyl radicals. Diffusable hydroxyl radicals produced from Fe-EDTA or Cu-phenanthroline complexes effect cleavage of the phosphodiester backbone of both DNA and RNA; cleavage of radiolabeled molecules can be easily analyzed on high-resolution polyacrylamide gels (*13, 14*). Protection against such cleavage through binding of a protein or formation of a higher order structure is detected as an area of reduced cleavage or footprint. These commonly used footprinting techniques may be regarded as *thermodynamic* since the radicals are typically generated over a 10−60 min time period

† This work was supported by the Natural Sciences and Engineering Research Council of Canada. S.G.C. is the recipient of a Walter C. Sumner Fellowship.

* To whom correspondence should be addressed. Phone/FAX: 416-978-8603; e-mail: amacmill@chem.utoronto.ca.

10.1021/bi992167e CCC: $19.00
Published on Web 12/11/1999

and thus are useful for examining a system at equilibrium. In studies on the folding of the Group I ribozyme, Latham and Cech (*14*) used Fe-EDTA as a thermodynamic structural probe and observed strong, magnesium-dependent protections in the folded state of the ribozyme.

The tremendous utility of radical footprinting as a technique of structure-probing has prompted efforts to develop *kinetic* radical footprinting techniques. Detailed studies of the folding of the L-21 *Sca*I ribozyme have been carried out using a synchroton X-ray source to produce hydroxyl radicals (*10, 11*). The generation of radicals on a 50−100 ms time scale allowed kinetic footprinting experiments to be performed which differentiated folding events occurring with rate constants between 0.02 and 2.7 s^{-1}. In agreement with the oligonucleotide hybridization/RNase H cleavage studies, these experiments demonstrated an ordered folding pathway for the Group I ribozyme. The most stable domain of the ribozyme, P4−P6, was shown to form very quickly with maximal protection from radical-induced cleavage observed within seconds of initiation of folding. This was followed by a series of slower events: protection of exterior helices of the ribozyme from radical-induced cleavage took place over the course of tens of seconds with the P3 and P9 regions being protected later in the folding pathway.

Our interest in the dynamics of RNA structure in several systems has prompted us to explore the application of kinetic footprinting reagents to the study of RNA folding. Here we describe the use of a simple and readily available reagent, peroxynitrous acid, as a tool for examining the folding pathway of a complex RNA: the *Tetrahymena* ribozyme. Kinetic footprinting of the magnesium-dependent folding of the ribozyme resulted in the identification of several slow steps in a folding pathway. The kinetics observed for these steps are consistent with those observed by synchrotron X-ray footprinting. Interestingly, we observe two distinct rates for protection of the P3 region of the RNA which may reflect transitions in this structure during the RNA folding. As well, none of the observed steps were as slow as the overall folding rate. This argues that the final folding to an active structure involves local rearrangements in a globally folded structure.

EXPERIMENTAL PROCEDURES

Materials

The pT7L-21 plasmid was provided by Dr. Jamie Williamson (Scripps Research Institute). *Sca*I restriction enzyme, nucleoside triphosphates, and ribonuclease inhibitor were from Pharamacia, T7 RNA polymerase was from Promega, calf intestinal alkaline phosphatase was from Boehringer Manheim, T4 polynucleotide kinase was from New England Biolabs, and yeast poly(A) polymerase was from Amersham Life Science. The 11 nucleotide L-21 *Sca*I substrate, CCCUCUAAAAA, was obtained from Cruachem. [γ-^{32}P]ATP (6000 Ci/mmol, 5 mCi/0.03 mL) and [α-^{32}P]cordycepin (5000 Ci/mmol, 250 μCi/0.025 mL) were purchased from New England Nuclear. Quiksep spin columns were purchased from Isolab Inc.

Methods

RNA Preparation. The pT7L-21 plasmid was digested for runoff transcription. Digestion reactions (200 μL) contained pT7L-21 plasmid (20 μg), *Sca*I (200 units), 70 mM Tris, pH 7.6, 10 mM $MgCl_2$, and 5 mM DTT and proceeded for 10 h at 37 °C. Reactions were then extracted with phenol/chloroform/isoamyl alcohol and chloroform/isoamyl alcohol and ethanol-precipitated. L-21 Group I ribozyme transcription reactions were performed under two different sets of conditions. To prepare RNA for measurement of overall folding kinetics or for experiments in which the RNA was to be 5′-end-labeled, transcriptions (0.5 mL) were performed for 6 h at 37 °C in 40 mM Tris (pH 8), 6 mM $MgCl_2$, 2 μM spermidine, 10 mM NaCl, and 10 mM DTT, using 1 mM nucleoside triphosphates, 20 units of ribonuclease inhibitor, 400 units of T7 RNA polymerase, and 10 μg of *Sca*I-digested pT7L-21 plasmid as template. For footprinting experiments with 3′-end-labeled RNA, we synthesized the ribozyme using conditions which produce transcripts with homogeneous 3′-ends (R. Collins and S. Hiley, submitted for publication): reactions (100 μL) containing 40 mM Tris-HCl (pH 7.9), 2 mM spermidine, 25 mM NaCl, 3 mM $MgCl_2$, 4 mM DTT, 1 mM nucleoside triphosphates, 5 μg of *Sca*I-digested pT7L-21 plasmid, and 400 units of T7 RNA polymerase were incubated for 1 h at 37 °C. Transcriptions were purified directly by denaturing 20% (19:1) PAGE. The transcript was visualized by UV shadowing, excised, and extracted with phenol/chloroform/isoamyl alcohol (200 μL) and 0.3 M NaOAc (pH 5.3, 400 μL) for 4 h at 37 °C. After extraction, polyacrylamide was removed by centrifugation through a paper-disk spin column. The filtrate was then extracted with chloroform/isoamyl alcohol and ethanol-precipitated. RNA was resuspended in 50 μL of TE and stored at −78 °C to minimize degradation.

Ribozyme 5′-End-Labeling. L-21 Group I ribozyme (300 pmol) was 5′-dephosphorylated with 3 units of calf intestinal alkaline phosphatase for 20 min in 25 μL reactions at 37 °C containing 50 mM Tris-HCl, 0.1 mM EDTA, followed by an additional 3 units of CIAP for 20 min. Reactions were then extracted with phenol/chloroform/isoamyl alcohol and chloroform/isoamyl alcohol followed by ethanol precipitation. L-21 Group I ribozyme labeling reactions (40 μL) contained 150 pmol of RNA, 70 mM Tris, pH 7.6, 10 mM $MgCl_2$, 5 mM DTT, 4 units of T4 polynucleotide kinase, and 6 μL of [γ-^{32}P]ATP and proceeded for 15 min at 37 °C. Reactions were then purified directly by denaturing 4% (19:1) PAGE. The transcript was visualized by autoradiography, excised, and extracted with phenol/chloroform/isoamyl alcohol (200 μL) and 0.3 M NaOAc (pH 5.3, 400 μL) for 4 h at 37 °C. After extraction, polyacrylamide was removed by centrifugation through a paper-disk spin column; the filtrate was then extracted with chloroform/isoamyl alcohol and ethanol-precipitated. RNA was resuspended in 50 μL of TE and stored as described above.

Ribozyme 3′-End-Labeling. Reactions (25 μL) were performed at 30 °C for 20 min and contained 20 mM Tris-HCl (pH 7.0), 50 mM KCl, 0.7 mM $MnCl_2$, 0.2 mM EDTA, 100 μg/mL acetylated BSA, 10% glycerol, 0.6 μM L-21 Group I ribozyme, 1500 units of yeast poly(A) polymerase, and 125 μCi of [α-^{32}P]cordycepin. The reactions were purified by denaturing PAGE; full-length RNA was isolated and stored as described above.

Substrate 5′-End-Labeling. L-21 Group I ribozyme substrate, CCCUCUAAAAA (Cruachem), labeling reactions (40

μL) contained 50 pmol of RNA, 70 mM Tris, pH 7.6, 10 mM $MgCl_2$, 5 mM DTT, 4 units of T4 polynucleotide kinase (New England Biolabs), and 2 μL of [γ-^{32}P]ATP (6000 Ci/mmol, 5 mCi/0.03 mL, New England Nuclear) and proceeded for 15 min at 37 °C. Reactions were then extracted with phenol/chloroform/isoamyl alcohol and chloroform/isoamyl alcohol followed by ethanol precipitation. RNA was resuspended in 50 μL of TE and stored as described above.

Endoribonuclease Activity Folding Assay. The rate of folding of the L-21 Group I ribozyme was assayed by its endoribonuclease activity (CCCUCUAAAAA + GTP → CCCUCU + pppGAAAAA) at 25 °C (*8*). Aliquots (10 μL) from a ribozyme stock solution (100 nM ribozyme, 80 mM NaCl, 10 mM $MgCl_2$, 50 mM NaH_2PO_4/Na_2HPO_4, pH 7) were combined with aliquots (10 μL, 1×10^5 cpm) of a substrate stock solution (32 nM 5′-end-labeled substrate, 80 mM NaCl, 10 mM $MgCl_2$, 50 mM NaH_2PO_4/Na_2HPO_4, pH 7, 1 mM GTP) at the indicated times (see Figure 1B) following $MgCl_2$ addition to the ribozyme stock solution. Reactions proceeded for 50 s before being quenched with an equal volume of stop solution (100 mM Na_2EDTA, 6.4 M urea, 0.4 mg/mL bromophenol blue, 0.4 mg/mL xylene cyanole, 0.4 M Tris base, 0.4 M boric acid). Reactions were then subjected to denaturing 20% (19:1) PAGE for 2 h at 30 mA. Gels were exposed to a Molecular Dynamics Phosphor Screen which was then scanned on a Molecular Dynamics Storm 860 Phosphorimager. Extents of reaction were quantitated (ImageQuant 5.0), and a plot of the normalized extent of reaction versus folding time was fitted to a first-order exponential (GraFit 3.00) using data from two experiments.

Potassium Peroxynitrite Synthesis. To a stirring ice-cooled aqueous solution (10 mL) containing 0.6 M (0.41 g) $NaNO_2$ and 3% H_2O_2 was added 0.5 M HCl (5 mL) followed immediately by a solution (5 mL) containing 400 μM (3.3 mg) diethylenetriaminepentaacetic acid and 1.6 M KOH. The resulting mixture was stirred for 5 min. Then MnO_2 (100 mg) was added and stirring continued for 20 min. Excess MnO_2 was removed by centrifugation (performed at 4 °C). Typical yields of potassium peroxynitrite were 80−130 mM by UV absorbance at 302 nM ($\epsilon = 1670\ M^{-1}$). A delay of even several seconds in the addition of the KOH/diethylenetriaminepentaacetic acid solution resulted in significantly lower yields of potassium peroxynitrite. The potassium peroxynitrite solution was then stored at −78 °C with no decrease in concentration after 6 months.

Peroxynitrous Acid Footprinting. L-21 Group I ribozyme folding was initiated by the addition of $MgCl_2$ (final concentration 10 mM) to a solution (final volume 20 μL) containing final concentrations of 80 mM NaCl, 50 mM NaH_2PO_4/Na_2HPO_4 (pH 7), and 50 nM 5′- or 3′-end-labeled ribozyme [$(0.5-3.0) \times 10^6$ cpm] at 25 °C. Footprinting was then effected by the addition of potassium peroxynitrite (1 μL, 80−130 mM) at the indicated times (see Figures 2 and 3). Footprinting reactions were allowed to proceed for 20 s before freezing on dry ice, followed by ethanol precipitation. Reactions [$(0.3-1.0) \times 10^6$ cpm] were then subjected to denaturing 6% (19:1) PAGE at 85 W (2.3 h for 5′-end-labeled RNA and 1.7 h for 3′-end-labeled RNA). Dried gels were exposed to a Molecular Dynamics Phosphor Screen which was then scanned on a Molecular Dynamics Storm 860 Phosphorimager. To calculate the fractional peroxynitrous acid protection (footprint), the background intensity (ImageQuant 5.0) was first subtracted, and a correction for differences in lane loading was applied. Then the intensity of a region at a given time was divided by the intensity of the same region at time zero. The resulting fractional intensities were normalized from 0 to 1. Using data averaged from three separate experiments, plots of normalized fractional protection versus folding time were fitted to a first-order exponential (using GraFit 3.00 and assuming that the observed protections were first-order processes; *8*, *10*, *11*). Rates of protection derived from this analysis are reported with an error representing one standard deviation at a 65% confidence level.

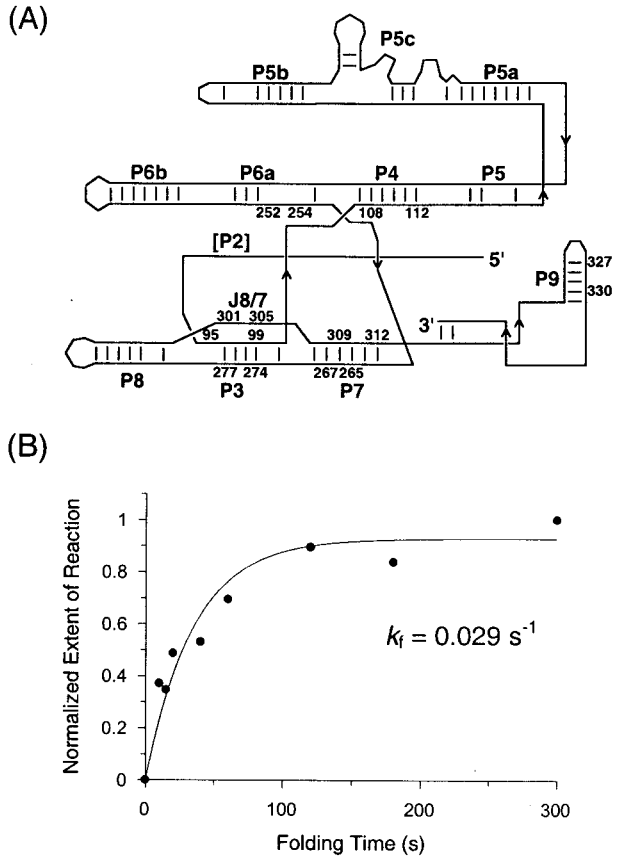

FIGURE 1: (A) Schematic (after ref *4*) of the secondary structure of the L-21 *Sca*I Group I ribozyme showing paired (P) regions and joining (J) sequences. Nucleotides referred to in this study are indicated. (B) Measurement of endoribonuclease activity of the ribozyme as a function of time following addition of Mg^{2+}. The observed activity is proportional to the amount of folded ribozyme. Under the conditions used in this study, the overall rate of folding, k_f, is $0.029 \pm 0.005\ s^{-1}$.

Size Standards—RNase T1 Ladder. Positions of hydroxyl radical induced RNA cleavage were determined by comparison to an RNase T1 cleavage ladder. RNase T1 cleavage reactions were carried out by adding 2.5 units of RNase T1 (Pharmacia) to a solution (50 μL, pH 5.0, 55 °C) containing 18 mM citric acid, 0.9 mM Na_2EDTA, 6.3 M urea, 100 nM 5′-end-labeled ribozyme (7.5×10^6 cpm), and 13.5 mg/mL tRNA. Reactions proceeded for 1 min and were then extracted with phenol/chloroform/isoamyl alcohol and chloroform/isoamyl alcohol followed by ethanol precipitation. Approximately 2×10^5 cpm were loaded per lane.

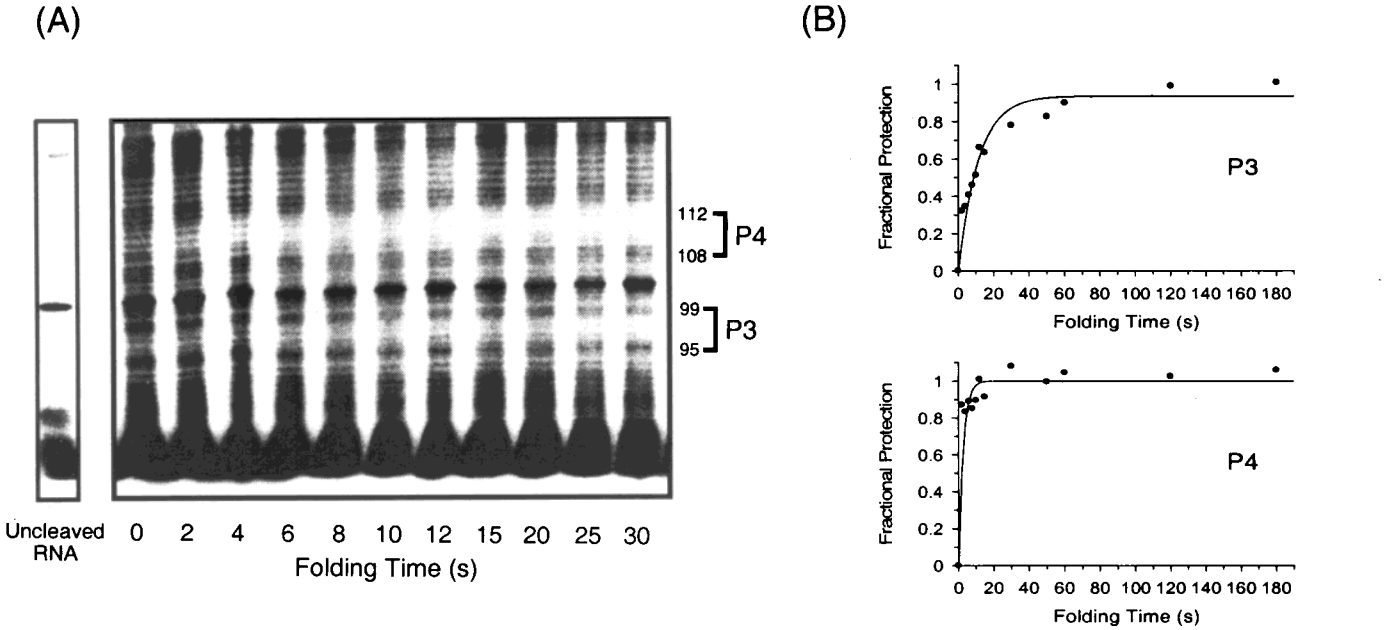

FIGURE 2: Kinetic footprinting of the folding pathway of the L-21 *Sca*I Group I ribozyme. (A) Denaturing PAGE analysis of 5′-end-labeled RNA treated with peroxynitrous acid at the indicated times following initiation of folding with Mg^{2+}; the protected nucleotides of P3 and P4 are indicated (see Figure 1A). (B) Relative protection of the P3 and P4 regions of the ribozyme as a function of folding time. The P3 and P4 regions were protected 60% and 80%, respectively, relative to unfolded RNA; protections over the indicated time course were normalized to these values.

RESULTS

Peroxynitrous acid has been demonstrated to be unstable in water at neutral pH, undergoing homolytic cleavage to generate hydroxyl radical and nitrogen dioxide (eq 1); the

$$KOONO \xrightarrow{H^+} HOONO \longrightarrow HO\bullet + NO_2\bullet$$

yield of reactive radical is around 10% with approximately 90% of the decomposition occurring by collapse of the radical pair to give nitric acid (*15*). We prepared aqueous solutions of peroxynitrous acid by oxidation of nitrous acid with hydrogen peroxide (*16*). The decompostion of peroxynitrous acid is rapid, taking place with a half-life of about 1 s at pH 7 or lower (*17*). We therefore found that care had to be taken at this stage in the preparation of the reagent: oxidation of the nitrous acid was immediately followed by basification with aqueous potassium hydroxide. The potassium salt of the acid is stable in basic solution. Protonation, by addition of the salt to a buffered solution, regenerates the unstable acid and thus serves as a trigger for hydroxyl radical production (eq 1). Disproportionation of excess hydrogen peroxide was effected by the addition of manganese oxide which could subsequently be removed by simple centrifugation. The yield of the resulting potassium peroxynitrite was determined by measuring its UV absorbance at 302 nm ($\epsilon = 1670\ M^{-1}$; *18*). Stock solutions which were 80−130 mM in reagent (representing a yield of 27−44%) and which were suitable for further experiments could be routinely prepared in this way. Aqueous solutions of potassium peroxynitrite were stored frozen at −78 °C and were found to be stable over a period of at least 6 months.

We synthesized the L-21 *Sca*I ribozyme by T7 runoff transcription from the cut plasmid pT7L-21 and assayed it for activity in the cleavage of a ^{32}P-labeled 11 nucleotide RNA substrate. Using this activity as an assay for magnesium-dependent folding of the ribozyme (*8*), we were able to observe a folding process taking place over several minutes with an observed rate of $0.029 \pm 0.005\ s^{-1}$ (Figure 1B).

Before performing kinetic footprinting experiments, we tested the reactivity of peroxynitrous acid with unfolded L-21 *Sca*I RNA. In initial experiments, we treated samples of 5′ ^{32}P end-labeled RNA with peroxynitrous acid and observed cleavage of the RNA at nucleotide resolution when analyzed by denaturing PAGE alongside hydroxide and RNase T1 ladders (data not shown). A final concentration of ∼5 mM peroxynitrous acid was found optimal; reactions performed with 10-fold less reagent resulted in minimal cleavage of the RNA.

We carried out our initial kinetic footprinting studies by the addition of freshly prepared potassium peroxynitrite to folding reactions containing ^{32}P 5′-end-labeled RNA at various time points following the addition of magnesium chloride. Reactions were desalted by precipitation and analyzed by denaturing gel electrophoresis (Figure 2A). Control cleavages with RNase T1 were carried out to create a G ladder and thus allow mapping of cleavage sites to specific regions of the ribozyme sequence. It was apparent that the addition of Mg^{2+} resulted in significant protection of portions of the ribozyme from radical-induced cleavage. The most signficant footprints observed were in the P3 and P4 helical regions; in the fully folded RNA, these were protected ∼60% and 80%, respectively, compared to the unfolded state. To assess the time and domain dependence of such cleavage, we quantified cleavages over specific regions and plotted these as a fraction of relative protection vs time (Figure 2B). Fitting the data for P3 protection to a first-order exponential allowed us to extract a rate constant of $0.09\ s^{-1}$ for protection of this region. Protection of P4 occurred too quickly for the accurate determination of a rate constant (see Table 1).

We next prepared prepared RNA for 3′-end-labeling and folding analysis. To produce a pool of RNA with homoge-

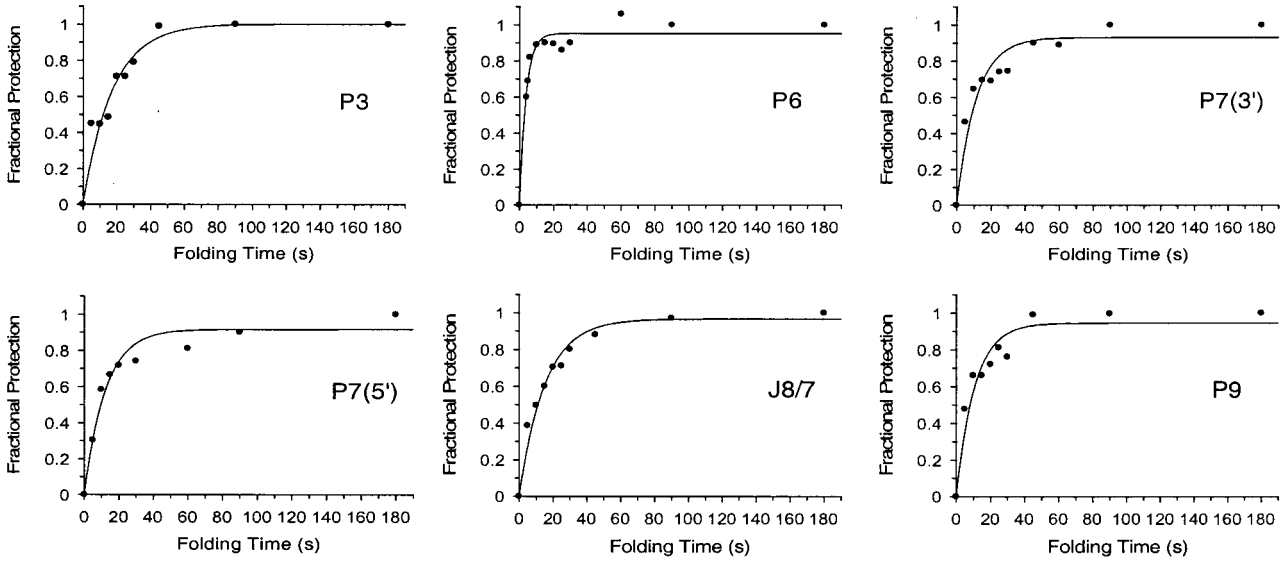

FIGURE 3: Relative protection of the P3, P6, P7, P9, and J8/7 regions of the L-21 *Sca*I Group I ribozyme in kinetic footprinting experiments performed with peroxynitrous acid using 3′-end-labeled RNA. All regions shown were protected ~50% relative to unfolded RNA; protections were normalized to this value to produce the plots shown. P7(5′) and P7(3′) refer to the 5′ and 3′ sides of the P7 helix.

Table 1: Peroxynitrous Acid Footprinting: First-Order Rate Constants for Folding of L-21 *Sca*I Group I Ribozyme at 25 °C

region[a]	nucleotides protected[a]	k (s^{-1})[b]
P3[c]	97−99	0.09 ± 0.01
P4[c]	108−112	−[e]
P3[d]	274−277	0.05 ± 0.01
P6[d]	252−255	0.27 ± 0.03
P7 (5′)[d]	265−267	0.08 ± 0.01
P7 (3′)[d]	309−312	0.09 ± 0.01
P9[d]	327−330	0.09 ± 0.02
J8/7[d]	301−305	0.07 ± 0.01

[a] See Figure 1; relative protection as a function of time was determined over the sequence indicated. [b] Reported errors are one standard derivation from the calculated value. [c] Determined using 5′-end-labeled RNA. [d] Determined using 3′-end-labeled RNA. [e] Not determined.

neous 3′-ends, we made use of a novel transcription protocol which significantly reduces n+1 transcription products (R. Collins and S. Hiley, submitted for publication). Using these conditions, we were able to directly synthesize RNA in which the "full-length" material was over 90% pure (as determined by RNase T1 analysis; data not shown).

Kinetic footprinting experiments with 3′-end-labeled RNA were carried out exactly as described for the 5′-end-labeled RNA and were analyzed by denaturing PAGE and quantified in the same manner. Protection from hydroxyl radical-induced cleavage, dependent on both divalent magnesium and time, was observed for several regions. The extent of protection observed was ~50% in all cases comparing fully folded to unfolded RNA. The specific protected regions were indentified using an RNase T1 ladder, and the extent of protection vs time was quantified (Figure 3). The resulting curves were fit to first-order exponentials to give rate constants between 0.05 and 0.27 s^{-1} (Table 1).

DISCUSSION

In this study, we have demonstrated the utility of peroxynitrous acid as a radical source for kinetic footprinting using the folding of the *Tetrahymena* intron as a model system. Kinetic footprinting has been well established as a tool for studying dynamics in complex RNA systems—most notably by an elegant series of studies on the folding pathway of the *Tetrahymena* intron using a synchrotron X-ray source to generate hydroxyl radicals. Hydroxyl radicals are attractive as reagents for probing the formation of complex RNA structures since their reaction is independent of sequence or formation of double-stranded structure. We were thus interested in utilizing a readily available reagent as a radical source for kinetic footprinting studies. Peroxynitrous acid has been demonstrated by Ingold and co-workers to produce hydroxyl radicals upon decomposition (*15*). It has also been shown that the cleavage products produced upon treatment of DNA with peroxynitrous acid comigrate with those produced by treatment with iron-EDTA (*19*) and therefore a hydroxyl radical initiated reaction cascade resulting in backbone scission is highly likely for the former process. Peroxynitrous acid has previously been used as a footprinting reagent to examine the *lac* repressor−DNA complex and also as a probe of tRNA structure (*16*, *20*). The methodology described here should find wide application in the elucidation of RNA folding pathways and the examination of RNA dynamics in complex systems. The reagent is easily prepared, and radical production is initiated by simple addition of reagent stock to a buffered solution. The half-life for generation of radicals is on the order of 1 s at neutral pH—thus, the reagent is suitable for examining processes occurring with half-lives as low as 3 s. The generation of radicals on the 100 ms time scale by synchrotron irradiation means that this method is superior for the study of very fast processes: nevertheless, many RNA folding events take place over the course of minutes and are thus amenable to studies using peroxynitrous acid.

We chose the L-21 *Tetrahymena* ribozyme, a 385 nucleotide sequence-specific endoribonuclease derived from a self-splicing Group I intron, as a model system for our studies. This RNA has been exceptionally well characterized biochemically, and the structures of several large fragments have been determined by X-ray crystallography. Most importantly,

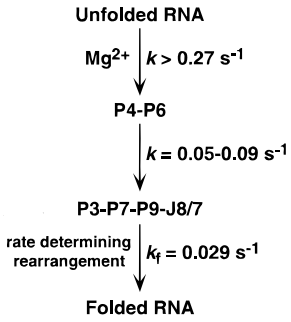

FIGURE 4: Partial hierarchy of the magnesium-dependent folding pathway of the L-21 *Sca*I Group I ribozyme. The overall rate of folding, k_f, derived from the folding/activity assay (Figure 1B; *8*) is half the rate of the slowest step observed by kinetic footprinting and corresponds to as yet uncharacterized rearrangements following formation of the global folded structure.

the folding pathway has been studied in detail using two independent methods: hybridization/cleavage and synchrotron hydroxyl radical footprinting.

Using a combination of 5′- and 3′-end-labeled RNAs, we were able to perform a kinetic footprinting analysis of the folding pathway of the Group I ribozyme as summarized in Table 1. Our data are in good qualitative agreement with the results of both oligonucleotide hybridization/cleavage and synchrotron hydroxyl radical footprinting. That is, the folding pathway of the Group I ribozyme proceeds through discrete intermediates (Figure 4) with early events such as formation of P4 taking place significantly faster (∼10-fold) than others (formation of P3, P7, and P9; protection of J8/7).

The rate constants derived from this study for protection of P3, P4, P7, P9, and J8/7 are in close agreement with those derived from synchrotron footprinting (Table 1; *11*) despite the fact that the present study was conducted at 25 °C while the synchrotron data were obtained at 42 °C. This suggests that the rate-determining step of folding is more temperature sensitive than the earlier, faster steps observed in this study: we are carrying out further kinetic footprinting experiments to test the temperature dependence of observed folding events.

Two separate rates (∼2-fold different) were observed for protection of the 5′ and 3′ sides of the P3 region. A similar observation was made in synchrotron-based footprinting studies and is suggestive of late rearrangements in the vicinity of P3 during the folding pathway (*10*, *11*, *21*). Pan and Woodson have provided convincing evidence for formation of alternate P3 structures during the folding of the *Tetrahymena* RNA (*21*), and this may be reflected in the differential protection rates of P3 reported here and in the synchrotron studies. It should be borne in mind that the reduced cleavage of a particular region of the RNA as visualized by the kinetic footprinting experiment reflects protection of that region from cleavage as opposed to the formation of a specific structure containing those nucleotides. Thus, a loosely formed structure could undergo a number of transitions on the path to a final folded entity.

Finally, although protection of P3, P7, P9, and J8/7 occurred with rates which were significantly slower than protection of P4, all of these rates were ∼2-fold faster than the overall rate of folding as determined in the folding/activity assay. This indicates that there is a later rate-determining step in the folding of the RNA than seen in these studies (*21*, *22*). It is possible that this step is refractive to analysis by the kinetic footprinting technique described here. Alternatively, adoption of the final folded structure may be involved with cofactor or substrate binding—a possibility we are actively pursuing.

This study has clearly demonstrated the usefulness of a readily available reagent, peroxynitrous acid, as a kinetic footprinting tool. Discrete rates of protection during the folding of the Group I intron were measured, providing a quantitative picture of the folding pathway of this molecule. Because the thermal generation of radicals from the peroxyacid takes place on a time scale of approximately 1 s, the fastest rates which can be measured are those for processes occurring with a half-life of around 3 s such as protection of the P6 region in the Group I ribozyme. Recent reports of radical generation from *N*-hydroxypyridinones by laser photolysis (*23*, *24*) suggest that these simple precursors might be used for production of radicals on the millisecond time scale, allowing investigation of even faster processes.

ACKNOWLEDGMENT

We are grateful to Vernon Anderson for calling our attention to peroxynitrous acid as a footprinting reagent, thank Shawna Hiley for providing RNA for 3′-labeling experiments, and thank Vanita Sood and Rick Collins for helpful discussions.

REFERENCES

1. Gesteland, R. F., Cech, T. R., and Atkins, J. F., Eds. (1999) in *The RNA World, 2nd Edition*, Cold Spring Harbor Laboratory, Cold Spring Harbor, NY.
2. Michel, F., and Westhof, E. (1990) *J. Mol. Biol. 216*, 585.
3. Cate, J. H., Gooding, A. R., Podell, E., Zhou, K., Golden, B. L., Kundrot, C. E., Cech, T. R., and Doudna, J. A. (1996) *Science 273*, 1678.
4. Golden, B. L., Gooding, A. R., Podell, E. R., and Cech, T. R. (1998) *Science 282*, 259.
5. Scott, W. G. (1998) *Curr. Opin. Struct. Biol. 8*, 720.
6. Wu, M., and Tinoco, I., Jr. (1998) *Proc. Natl. Acad. Sci. U.S.A. 95*, 11555.
7. Szewczak, A. A., Ortoleva-Donnelly, L., Ryder, S. P., Moncoeur, E., and Strobel, S. A. (1998) *Nat. Struct. Biol. 5*, 1037.
8. Zarrinkar, P. P., and Williamson, J. R. (1994) *Science 265*, 918.
9. Zarrinkar, P. P., and Williamson, J. R. (1996) *RNA 2*, 564.
10. Sclavi, B., Woodson, S., Sullivan, M., Chance, M. R., and Brenowitz, M. (1997) *J. Mol. Biol. 266*, 144.
11. Sclavi, B., Sullivan, M., Chance, M. R., Brenowitz, M., and Woodson, S. A. (1998) *Science 279*, 1940.
12. Walter, N. G., Burke, J. M., and Millar, D. P. (1999) *Nat. Struct. Biol. 6*, 544.
13. Chen, C.-H. B., and Sigman, D. S. (1988) *J. Am. Chem. Soc. 110*, 6570.
14. Latham, J. A., and Cech, T. R. (1989) *Science 245*, 276.
15. Richeson, C. E., Mulder, P., Bowry V. W., and Ingold, K. U. (1998) *J. Am. Chem. Soc. 120*, 7211.
16. King, P. A., Jamison, E., Strahs, D., Anderson, V. E., and Brenowitz, M. (1993) *Nucleic Acids Res. 21*, 2473.
17. Beckman, J. S., Beckman, T. W., Chen, J., Marshall, P. A., and Freeman, B. A. (1990) *Proc. Natl. Acad. Sci. U.S.A. 87*, 1620.
18. Hughes, M. N., and Nicklin, H. G. (1968) *J. Chem. Soc. A*, 450.
19. King, P. A., Anderson, V. E., Edwards, J. O., Gustafson, G., Plumb, R. C., and Suggs, J. W. (1993) *J. Am. Chem. Soc. 114*, 5430.

20. Götte, M., Marquet, R., Isel, C., Anderson, V. E., Keith, G., Gross, H. J., Ehresmann, B., and Heumann, H. (1996) *FEBS Lett. 390,* 226.
21. Pan, J., and Woodson, S. A. (1998) *J. Mol. Biol. 280,* 597.
22. Rook, M. S., Treiber, D. K., and Williamson, J. R. (1998) *J. Mol. Biol. 281,* 609.
23. Aveline, B. M., Kochevar, I. E., and Redmond, R. W. (1996) *J. Am. Chem. Soc. 118,* 10124.
24. Aveline, B. M., Kochevar, I. E., and Redmond, R. W. (1996) *J. Am. Chem. Soc. 118,* 10113.

BI992167E